Cancer Cell
Article

Loss of p21 Permits Carcinogenesis from Chronically Damaged Liver and Kidney Epithelial Cells despite Unchecked Apoptosis

Holger Willenbring,[1,2,*] Amar Deep Sharma,[1,2] Arndt Vogel,[3,6] Andrew Y. Lee,[1] Andreas Rothfuss,[3,7] Zhongya Wang,[4,5] Milton Finegold,[8] and Markus Grompe[3,4,5]
[1]Institute for Regeneration Medicine
[2]Department of Surgery, Division of Transplantation
University of California, San Francisco, San Francisco, CA 94143, USA
[3]Department of Molecular and Medical Genetics
[4]Papé Family Pediatric Research Institute
[5]Oregon Stem Cell Center
Oregon Health & Science University, Portland, OR 97239, USA
[6]Klinik für Gastroenterologie, Hepatologie und Endokrinologie, Medizinische Hochschule Hannover, 30625 Hannover, Germany
[7]Bayer Schering Pharma AG, 13353 Berlin, Germany
[8]Department of Pathology, Texas Children's Hospital, Houston, TX 77030, USA
*Correspondence: willenbringh@stemcell.ucsf.edu
DOI 10.1016/j.ccr.2008.05.004

SUMMARY

Accumulation of toxic metabolites in hereditary tyrosinemia type I (HT1) patients leads to chronic DNA damage and the highest risk for hepatocellular carcinomas (HCCs) of any human disease. Here we show that hepatocytes of HT1 mice exhibit a profound cell-cycle arrest that, despite concomitant apoptosis resistance, causes mortality from impaired liver regeneration. However, additional loss of p21 in HT1 mice restores the proliferative capabilities of hepatocytes and renal proximal tubular cells. This growth response compensates cell loss due to uninhibited apoptosis and enables animal survival but rapidly leads to HCCs, renal cysts, and renal carcinomas. Thus, p21's antiproliferative function is indispensable for the suppression of carcinogenesis from chronically injured liver and renal epithelial cells and cannot be compensated by apoptosis.

INTRODUCTION

DNA-damaged cells are prone to malignant transformation and are therefore frequently aborted by apoptosis. Alternatively, if the damage is limited, cell survival and restoration of genomic integrity might be favorable. This requires temporary cell-cycle arrest and protection from apoptosis while DNA repair is occurring. Remarkably, both antiproliferative as well as antiapoptotic functions are combined in the cell-cycle regulator p21 (Gartel and Tyner, 2002). Since disabled apoptosis is assumed to be an adjuvant of genetic alterations, especially if the DNA-damaging stimulus persists, it has been suggested that the antiapoptotic effect of p21 could provide the grounds for carcinogenesis (Zhivotovsky and Kroemer, 2004). Therefore, sensitization toward apoptosis by inhibition of p21 may be a powerful strategy for the treatment of cancer (Weiss, 2003). However, p21 was originally identified as the effector of p53's cell-cycle inhibitory capacity, and, since unrestricted proliferation is another promoter of cancer (Zhivotovsky and Kroemer, 2004), the interplay of apoptosis and proliferation in p21-deficient cancer cells

SIGNIFICANCE

p53 prevents carcinogenesis by inducing cell-cycle arrest or apoptosis. The antiproliferative effect of p53 is mediated by p21, which also has antiapoptotic function to enable restoration of genomic integrity. Apoptosis resistance has been recognized as a major carcinogenic factor, and attenuation of p21 may enhance the effectiveness of chemotherapy. Controversy exists as to whether the cancer-suppressing effect of p53 is mainly attributable to its cell-cycle inhibitory or apoptosis-inducing capacity. Here we show that the antiproliferative function of p21 is indispensable in cancer-prone epithelial tissues such as liver and kidney. Apoptosis alone fails to prevent carcinogenesis from chronically injured p21-deficient cells. Our results highlight the essential role of cell-cycle control in intrinsic suppression and targeted therapy of cancer.

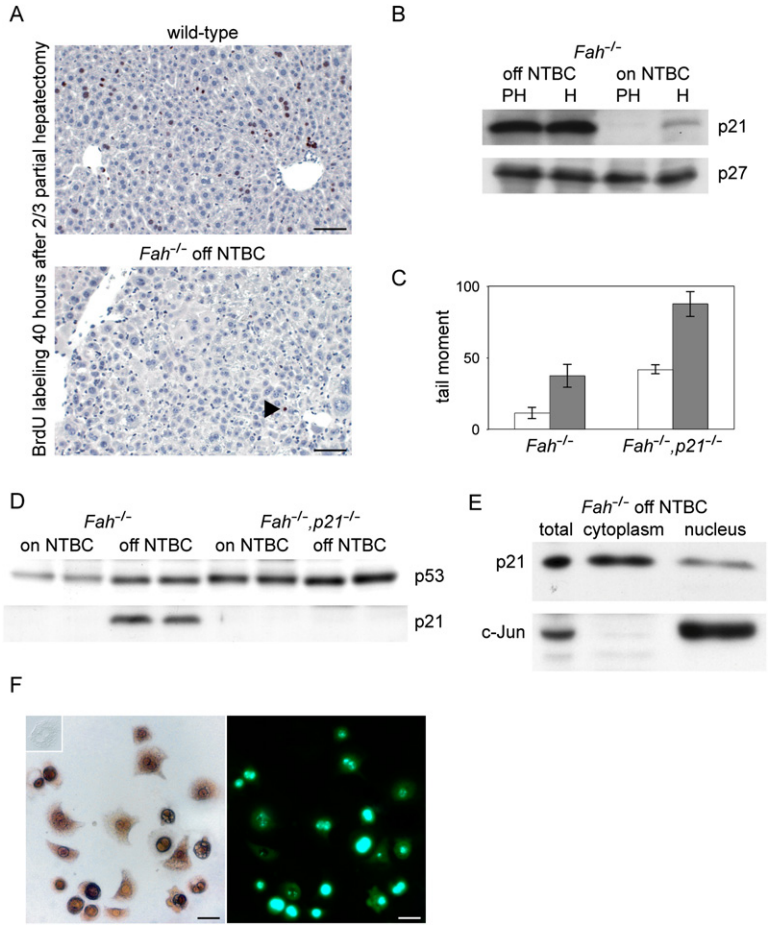

Figure 1. Fah Deficiency Causes Cell-Cycle Arrest Associated with DNA Damage and Induction of p21

(A) In contrast to wild-type cells (upper panel), Fah-deficient hepatocytes (lower panel) refrain from entry into S phase in response to 2/3 partial hepatectomy (PH), as evident from lack of BrdU labeling (brown, arrowhead in lower panel). Scale bars = 100 μm.

(B) p21 but not p27 protein is induced in $Fah^{-/-}$ mice after 2 weeks of NTBC withdrawal. p21 levels due to Fah deficiency markedly exceed those associated with the physiological halt of liver regeneration 72 hr after PH (H) in $Fah^{-/-}$ mice on NTBC. p21 protein levels are maximally induced in $Fah^{-/-}$ mice off NTBC for 2 weeks since they fail to increase after further stimulation by PH.

(C) Comet assay shows that NTBC withdrawal (gray columns) causes DNA damage (tail moment) in $Fah^{-/-}$ and $Fah^{-/-}$, $p21^{-/-}$ livers. $Fah^{-/-}$,$p21^{-/-}$ mice exhibit increased levels of DNA damage both on (white columns) and off NTBC. Error bars represent mean ± SD.

(D) DNA damage in $Fah^{-/-}$ and even more so in $Fah^{-/-}$,$p21^{-/-}$ hepatocytes is reflected by induction of p53.

(E and F) p21 protein induced by Fah deficiency is distributed between cytoplasm and nucleus as evident from western blot comparison to c-Jun, which is strictly limited to the nucleus (E), and p21 immunocytochemistry (brown, left panel in [F]) on plated hepatocytes costained for DNA with SYBR green I (green, right panel in [F]). Inset in left panel of (F) shows absence of p21 in a $Fah^{-/-}$,$p21^{-/-}$ hepatocyte. Scale bars = 25 μm.

remains to be elucidated before such therapeutic strategies can be pursued. In particular, regenerative capabilities such as those inherent to the liver must be rigorously controlled. In chronic liver diseases, accumulation of DNA damage results in dysplastic hepatocytes that eventually escape cancer control mechanisms and progress to hepatocellular carcinomas (HCCs) (Bruix et al., 2004). For example, the chronic liver injury inflicted by hereditary tyrosinemia type I (HT1) is associated with the highest risk for HCCs of any human disease (Russo and O'Regan, 1990). HT1 is due to mutations in the gene encoding fumarylacetoacetate hydrolase (Fah), the enzyme that completes tyrosine degradation, leading to accumulation of metabolites such as fumarylacetoacetate (FAA), which is a potent mutagenic agent (Jorquera and Tanguay, 1997). Accumulation of FAA can be prevented by blocking proximal tyrosine degradation with the drug 2-(2-nitro-4-trifluoromethylbenzoyl)-1,3-cyclohexanedione (NTBC) (Holme and Lindstedt, 2000). Unfortunately, NTBC therapy does not appear to be completely effective since both Fah-deficient mice and humans have been shown to develop hepatocyte dysplasias that potentially give rise to HCCs (Al-Dhalimy et al., 2002; Grompe et al., 1995; van Spronsen et al., 2005). Apart from the liver, Fah is specifically expressed in kidney proximal tubular cells, which have regenerative capabilities similar to hepatocytes. Modeling the chronic cell injury inherent to most human disease states, we identify p21's antiproliferative activity as essential for cell-cycle arrest and prevention of carcinogenesis in hepatocytes and renal proximal tubular cells. While apoptosis resistance maintained by p21 might contribute to dysplastic transformation of DNA-damaged liver and kidney epithelial cells, induced apoptosis following loss of p21 clearly fails to sufficiently eliminate cancer-initiating cells.

RESULTS

Failed Regeneration of Fah-Deficient Hepatocytes Is Associated with DNA Damage and Induction of p21

Fah-deficient mice taken off the drug NTBC mimic both the liver failure and kidney pathology of the human disease (Grompe et al., 1993) and have been shown to provide a strong selective environment for Fah-expressing cells (Overturf et al., 1996). We hypothesized that repopulation of the mutant host liver with wild-type donor cells requires either substantial cell death (Mallet et al., 2002) or an impaired proliferative response (Guo et al., 2002) in Fah-deficient hepatocytes. We previously showed that Fah-deficient hepatocytes (Vogel et al., 2004) as well as renal proximal tubular cells (Luijerink et al., 2004) are not susceptible to cell death but rather display a profound apoptosis-resistance phenotype. Therefore, to test whether positive selection of Fah-expressing cells is facilitated by inhibited proliferation of Fah-deficient hepatocytes, we performed labeling studies with 5-bromo-2-deoxyuridine (BrdU) after 2/3 partial hepatectomy (PH) (Greene and Puder, 2003) in $Fah^{-/-}$ mice that had been off NTBC for 2 weeks. Surprisingly, no BrdU-labeled hepatocytes could be detected at 40 hr, the time point with the largest number of hepatocytes in S phase after PH in mice (Mitchell et al., 2005) (Figure 1A).

Hepatocyte proliferation was not only delayed but blocked in these animals, as they showed no signs of liver regeneration and invariably died from liver failure within 4 days after PH (data not shown).

To identify genes instrumental in the cell-cycle arrest of Fah-deficient hepatocytes, we performed microarray analyses on liver samples from wild-type and $Fah^{-/-}$ mice on or off NTBC for 2 weeks (Table 1; see also Figure S1A available online). As reported previously (Luijerink et al., 2003), Fah deficiency affected the expression of a large number of genes including proliferation-associated genes such as *Ki67*, c-*jun*, and c-*myc*. However, within the cluster of genes that regulate cell-cycle progression, p21 mRNA (Table 1) as well as protein (Figure 1B) levels were most significantly induced after NTBC withdrawal.

Wild-type mouse liver has undetectable levels of p21 mRNA and protein (Albrecht et al., 1998), but high quantities are common in liver diseases caused by toxic agents (Bartosiewicz et al., 2001) or viral infections (Wagayama et al., 2001). This induction of p21 is most likely due to DNA damage, and FAA, the accumulating substrate for Fah, is known to be a potent oxidizing agent that leads to genomic instability in vitro (Jorquera and Tanguay, 1997, 2001). To assess the DNA-damaging effect of FAA in vivo, we performed comet assay (Singh et al., 1988) on liver samples from $Fah^{-/-}$ mice after 2 weeks of NTBC withdrawal. The tail moment in these analyses indicated that Fah deficiency was associated with profound DNA damage (Figure 1C). Interestingly, and in accordance with the increased late-onset cancer incidence of $p21^{-/-}$ mice (Martin-Caballero et al., 2001), animals deficient in both Fah and p21 ($Fah^{-/-}$,$p21^{-/-}$) showed increased levels of DNA damage not only off but also on NTBC. Elevated levels of p53 mRNA and protein were also present in $Fah^{-/-}$ livers, and therefore, in analogy to findings in human HCCs (Shi et al., 2000), the activation of p21 was most likely mediated by this classical pathway (Table 1; Figure 1D).

Previously, the antiapoptotic and antiproliferative activities of p21 have been correlated with its localization in the cytoplasm or the nucleus, respectively (Zhou et al., 2001). In Fah deficiency, p21 was abundant in both cellular compartments (Figures 1E and 1F). Thus, we wished to determine whether the cell-cycle arrest and apoptosis-resistance phenotype (Vogel et al., 2004) of Fah-deficient hepatocytes are dependent on p21.

Cell-Cycle Arrest of Fah-Deficient Hepatocytes Is Caused by Induced p21

Microarray analyses and cell-cycle distribution of $Fah^{-/-}$ hepatocytes after NTBC withdrawal were suggestive of cell-cycle inhibition by p21 (Table 1; Figure S1B). To test this, livers of $Fah^{-/-}$ and $Fah^{-/-}$,$p21^{-/-}$ mice that were off NTBC for 2 weeks and had received oral BrdU throughout the second week were compared. $Fah^{-/-}$,$p21^{-/-}$ livers showed marked proliferation of hepatocytes, whereas $Fah^{-/-}$ or wild-type livers contained very few BrdU-labeled cells (Figure 2A). Similar results were obtained with Ki67 (a general proliferation marker) (Figure 2B; Figure S2) and phosphorylated histone H3 (a mitosis-specific antigen) (Figure 2C) staining. Hence, p21 is needed to block hepatocyte proliferation after DNA damage inflicted by Fah deficiency.

Table 1. Hepatic Gene Expression Analysis of Wild-Type Compared to $Fah^{-/-}$ or $Fah^{-/-}$,$p21^{-/-}$ Mice after Two Weeks of NTBC Withdrawal

	Wild-Type	$Fah^{-/-}$ off NTBC	$Fah^{-/-}$,$p21^{-/-}$ off NTBC
p21	●◖	●●●	n/a
p53	●◖	●●	●●
p15	●	●●	●●
p16	●	●	●
p19[a]	●◖	●◖	●●
p27	●	●	●
Ki67[a]	●	●◖	●●◖
c-*jun*	●●	●●◖	●●◖
c-*myc*	●●	●●◖	●●◖
Cyclin A2[a]	●●	●●	●●◖
Cyclin B1[a]	●	●	●●◖
Gadd45a	●	●●	●●
Mdm2	●●	●●●	●●●
Apaf-1	●◖	●●	●●
Bax	●●◖	●●●	●●●
Rtp801	●◖	●●◖	●●◖
Puma	●●	●●	●●
Noxa[a]	●	●	●●
Afp	●◖	●●●◖	●●●◖
Albumin	●●●●	●●●●	●●●●

Gene expression levels are shown on a logarithmic scale: 10E(number of ●, with ◖ = ~0.5). The effect of NTBC on hepatic gene expression is restricted to Fah deficiency (data not shown). Hence, gene expression levels in wild-type mice on water represent findings in wild-type, $Fah^{-/-}$, and $Fah^{-/-}$,$p21^{-/-}$ mice on NTBC. Raw microarray data are provided in Figure S1A.

[a] Gene differentially expressed between $Fah^{-/-}$ and $Fah^{-/-}$,$p21^{-/-}$ mice.

$Fah^{-/-}$ mice invariably die from liver failure due to extensive hepatocellular necrosis accompanied by progressive weight loss within 8 weeks after NTBC withdrawal (Grompe et al., 1995). When NTBC was discontinued in $Fah^{-/-}$,$p21^{-/-}$ mice, their weight loss at first paralleled that of their $Fah^{-/-}$ littermates but then reached a plateau between 5 and 6 weeks (data not shown). Surprisingly, after 6 weeks of NTBC withdrawal, $Fah^{-/-}$,$p21^{-/-}$ animals began to regain their weight and, most importantly, survived more than 16 weeks of NTBC withdrawal (Figure 2D). This recovery was not reflected by normalization of serum liver function tests (data not shown), and we believe that the recovery of $Fah^{-/-}$,$p21^{-/-}$ mice is due to continuous liver regeneration, which maintains a critical level of liver function and allows subsequent metabolic adaptation. Some of the weight gain, however, was due to an increasing liver tumor burden (see below), and the animals eventually had to be euthanized. These results show that p21 is the key protein establishing and maintaining cell-cycle arrest in Fah deficiency and that blocked hepatocyte proliferation resulting in insufficient hepatocellular mass contributes to lethality in this disease. Interestingly, by performing PH in $Fah^{-/-}$ mice at various time points after NTBC withdrawal, we found that p21 must be maximally induced in order to counteract the strong regenerative stimuli elicited by PH (Michalopoulos

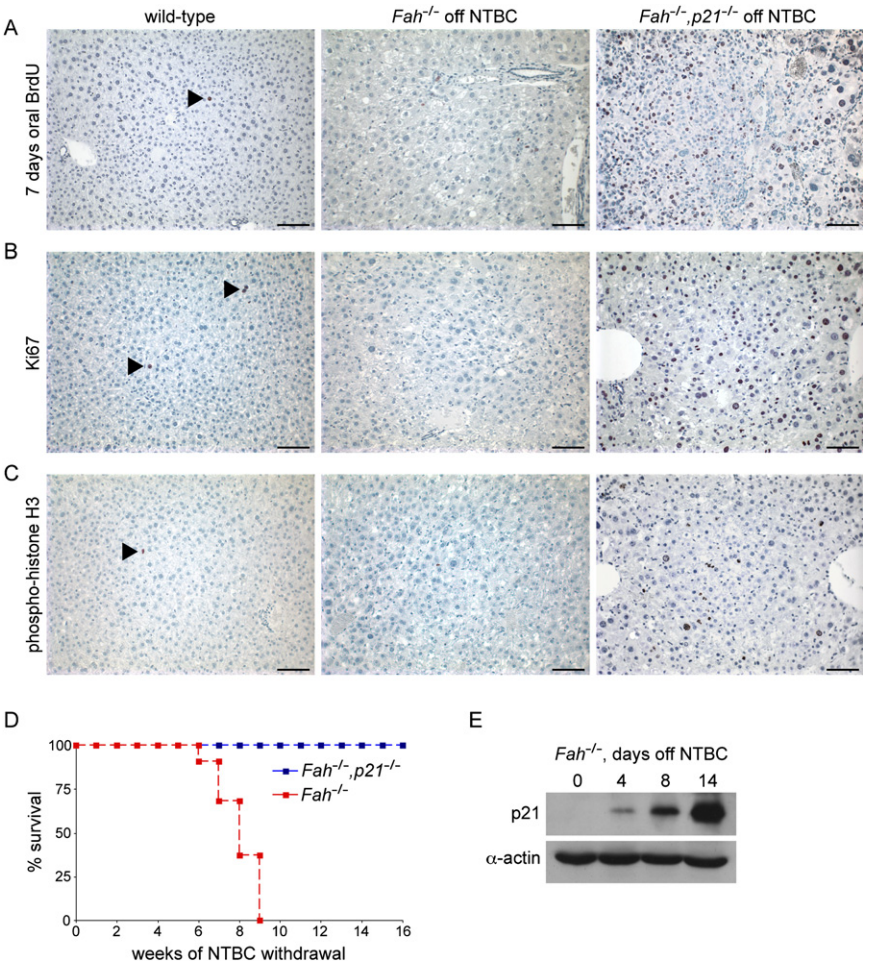

Figure 2. p21 Represses the Regenerative Response of Hepatocytes to Cell Damage Inflicted by Fah Deficiency

(A) Wild-type liver (left panel) contains very few proliferating (brown, BrdU labeling) hepatocytes (arrowhead). Upon NTBC withdrawal, $Fah^{-/-}$ hepatocytes (middle panel) fail to enter the S phase of the cell cycle, whereas $Fah^{-/-}$,$p21^{-/-}$ hepatocytes (right panel) show massive proliferation. Note dysplasia of $Fah^{-/-}$ and $Fah^{-/-}$,$p21^{-/-}$ hepatocytes off NTBC compared to wild-type cells. Scale bars = 100 μm.

(B and C) Immunohistochemistry (brown staining) for Ki67 (B) and phosphorylated histone H3 (C) show that despite liver injury induced by NTBC withdrawal, $Fah^{-/-}$ hepatocytes (middle panels) exhibit a proliferation arrest similar to wild-type cells (arrowheads, left panels) that is lifted in livers deficient in both Fah and p21 (right panels). Progression of $Fah^{-/-}$,$p21^{-/-}$ hepatocytes into the G2 and M phases of the cell cycle is apparent from both Ki67 (right panel in [B]) and phosphorylated histone H3 (right panel in [C]) staining. Quantification of Ki67-labeled hepatocytes is provided in Figure S2. Scale bars = 100 μm.

(D) Kaplan-Meier plot shows that $Fah^{-/-}$,$p21^{-/-}$ mice (blue line), but not their $Fah^{-/-}$ littermates (red line), survive beyond the critical phase of NTBC withdrawal. Ten mice were analyzed for each genotype.

(E) The cell-cycle inhibitory function of p21 in hepatocytes is dose dependent. Fourteen days after NTBC withdrawal, p21 protein levels are maximally induced. These p21 protein levels are needed for suppression of hepatocyte proliferation in $Fah^{-/-}$ mice after PH, as levels of p21 protein found after 4 or 8 days off NTBC fail to prevent liver regeneration (data not shown). Three mice were analyzed for each time point, and a representative western blot is shown. α-actin serves as loading control.

and DeFrances, 1997) (Figure 2E). Similarly, threshold p21 levels might be needed to antagonize the oncogenic gene expression in hepatocytes injured by Fah deficiency (Table 1).

Apoptosis Resistance of Fah-Deficient Hepatocytes Is p21 Dependent

Upon NTBC withdrawal, $Fah^{-/-}$ hepatocytes acquire profound resistance to multiple death triggers (Vogel et al., 2004). In contrast to this finding, TdT-mediated dUTP nick-end labeling (TUNEL) revealed many apoptotic hepatocytes in liver sections from $Fah^{-/-}$,$p21^{-/-}$ mice 2 weeks after NTBC discontinuation (Figure 3A). Apoptosis promoters known to be transcriptionally regulated by p53 such as Apaf-1, Bax, and Puma were moderately induced by Fah deficiency regardless of p21 status, with the exception of Noxa, which appeared to be repressed in $Fah^{-/-}$ hepatocytes and was highly expressed in $Fah^{-/-}$,$p21^{-/-}$ cells (Table 1). These results suggest that transcriptional repression of Noxa may be a key factor in apoptosis resistance caused by p21 induction. Accordingly, $Fah^{-/-}$,$p21^{-/-}$ but not $Fah^{-/-}$ mice showed massive apoptotic hepatocyte death following intraperitoneal injection of a monoclonal antibody that binds and activates Fas antigen (Jo2) (Figure 3B), which was accompanied by activation of caspase-3 (Figure 3C). These findings show that p21 causes the hepatocyte apoptosis resistance observed in Fah deficiency (Figure 3D). Remarkably, $Fah^{-/-}$,$p21^{-/-}$ mice survived by compensating hepatocyte loss due to Fas-mediated apoptosis with increased mitotic divisions (Figure 3E).

p21 Is Needed to Prevent Formation of Liver Cancer from Chronically Injured Hepatocytes

Apoptosis resistance and persistent proliferation of hepatocytes with damaged DNA have both been recognized as key factors in formation of HCCs (Montalto et al., 2002). Since p21 is capable of counteracting both cell death and cell division, its loss could result in either increased or decreased tumor formation, depending on which function is dominant. To first determine p21's impact on early cancer-initiating events, we examined livers of $Fah^{-/-}$ and $Fah^{-/-}$,$p21^{-/-}$ mice that had been off NTBC for 2 weeks for the expression of α-fetoprotein (AFP) (Table 1; Figures 4A–4C). AFP is expressed during liver development but is repressed in adult liver (Figure 4A). AFP is upregulated in 80% of human HCCs, but its expression is initiated in dysplastic hepatocytes that are precancerous (Montalto et al., 2002). Histological evaluation showed a similar frequency of AFP-positive

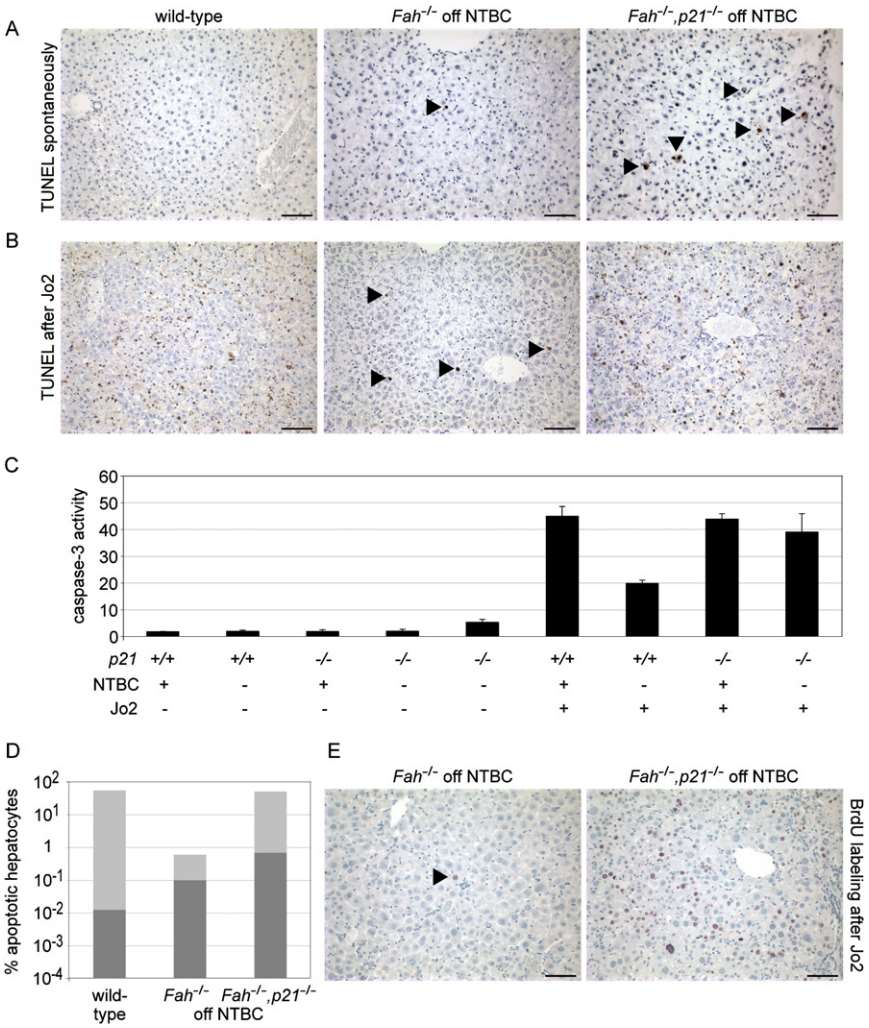

Figure 3. Apoptosis Resistance Inherent to Fah Deficiency Depends on p21

(A and B) In contrast to wild-type (left panels) or $Fah^{-/-}$ (middle panels) mice, $Fah^{-/-}$,$p21^{-/-}$ (right panels) animals exhibit increased numbers of TUNEL-positive hepatocytes (brown, arrowheads) after 2 weeks off NTBC (A), which can be further increased by application of a monoclonal antibody (Jo2) recognizing Fas (B).

(C) Hepatic apoptosis response in Fah-deficient mice depends on *p21* and NTBC status. Spontaneous caspase-3 activation is detectable in liver lysates from $Fah^{-/-}$,$p21^{-/-}$ mice off NTBC for 4 weeks (column 5) but not 2 weeks (column 4). In contrast, caspase-3 activation is undetectable in liver lysates from $Fah^{-/-}$,$p21^{-/-}$ and $Fah^{-/-}$ mice on NTBC (columns 3 and 1) or $Fah^{-/-}$ mice after 2 or 4 weeks of NTBC withdrawal (column 2). Jo2 injection induces massive caspase-3 activation in both $Fah^{-/-}$ and $Fah^{-/-}$,$p21^{-/-}$ mice on NTBC (columns 6 and 8). $Fah^{-/-}$ mice off NTBC show resistance to Jo2-induced apoptosis (column 7) that is abrogated in $Fah^{-/-}$,$p21^{-/-}$ mice off NTBC (column 9). Error bars represent mean ± SD.

(D) Quantification of the percentage of TUNEL-positive hepatocytes in untreated (dark gray columns) and Jo2-injected (light gray columns) mice.

(E) Injection of Jo2 is followed by BrdU labeling (brown staining) of many $Fah^{-/-}$,$p21^{-/-}$ hepatocytes (right panel), while very few $Fah^{-/-}$ hepatocytes (left panel, arrowhead) exhibit compensatory proliferation.

Three mice were analyzed for each genotype and treatment regimen. Representative stainings are shown, and corresponding H&E stainings are provided in Figure S3. Scale bars = 100 μm.

hepatocytes in $Fah^{-/-}$ and $Fah^{-/-}$,$p21^{-/-}$ mice (Figures 4B and 4C). AFP expression is tightly correlated with genomic instability in dysplastic hepatocytes and HCCs in mice (Calvisi et al., 2004). Therefore, p21's impact on genomic stability (Figure 1C) did not suffice to prevent dysplastic changes. However, while only dysplastic hepatocytes but no tumors were found in $Fah^{-/-}$ controls, all $Fah^{-/-}$,$p21^{-/-}$ mice developed multiple HCCs by 7–8 weeks after NTBC withdrawal (Figures 4D–4F). Histologically, these HCCs were equivalent to human HCCs of WHO grade 2–3 (Hirohashi et al., 2000). Molecular analyses revealed that these HCCs retained p53 function and induced expression of other cell-cycle regulators including p15, p16, and p19, which suggests a predominant role of p21's cell-cycle inhibitory function in liver cancer prevention (Figures S4A and S4B).

$Fah^{-/-}$ mice die of liver failure at around 8 weeks after NTBC withdrawal (Figure 2D). To compare tumor onset in $Fah^{-/-}$ and $Fah^{-/-}$,$p21^{-/-}$ mice under less acute conditions, we treated cohorts of mice with 5% of the normal NTBC dose. This leads to HCCs in $Fah^{-/-}$ mice within 1 year (Al-Dhalimy et al., 2002; Grompe et al., 1995). In contrast, $Fah^{-/-}$,$p21^{-/-}$ mice developed HCCs after only 8 weeks on low-dose NTBC. Although these tumors were smaller and fewer than in $Fah^{-/-}$,$p21^{-/-}$ mice completely off NTBC, they exhibited the same malignant phenotype (Figure S4C). Taken together, under conditions mimicking chronic human liver disease, the antiproliferative effect of p21 appears to be more important for prevention of HCCs than its antiapoptotic function.

Chronically Injured Renal Proximal Tubular Cells Give Rise to Cysts and Cancer in the Absence of p21

In addition to hepatocytes, the complete tyrosine degradation pathway including Fah is also expressed in proximal tubular epithelial cells in the kidney (Grompe et al., 1993). In the embryonic kidney, the growth-inhibitory effect of polycystin-1, the gene product of *Pkd1*, has been suggested to be mediated by transcriptional activation of p21 (Bhunia et al., 2002). Loss of polycystin-1 results in renal cyst formation that begins at embryonic day 15 in proximal tubular cells and progresses to replace the entire renal parenchyma by day 8 postpartum (Lu et al., 1997). Therefore, the renal phenotypes of $Fah^{-/-}$,$p21^{-/-}$ and $Fah^{-/-}$ mice were compared. In mice lacking only Fah, NTBC withdrawal resulted in renal tubular injury with aminoaciduria and mild kidney enlargement (data not shown) (Grompe et al., 1993). In contrast, $Fah^{-/-}$,$p21^{-/-}$ mice developed macroscopically detectable

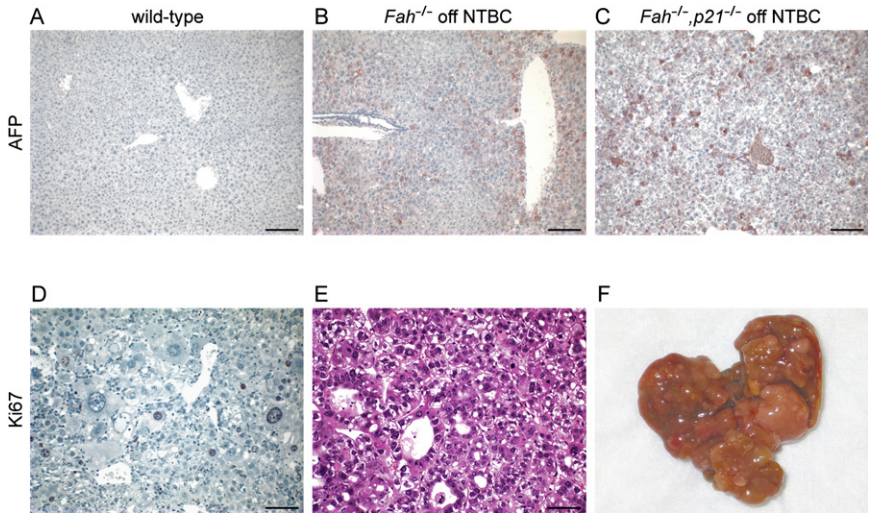

Figure 4. DNA-Damaged Hepatocytes Give Rise to Liver Cancer in the Absence of p21

(A–C) α-fetoprotein (AFP) immunohistochemistry (brown staining) indicates that wild-type livers (A) lack dysplastic hepatocytes while similar numbers of these cells are present in $Fah^{-/-}$ (B) and $Fah^{-/-}$, $p21^{-/-}$ (C) mice off NTBC. Scale bars = 100 μm.

(D) Ki67 immunohistochemistry (brown staining) marking proliferation of dysplastic hepatocytes in a $Fah^{-/-}$,$p21^{-/-}$ mouse off NTBC. Scale bar = 50 μm.

(E) Representative H&E staining of WHO grade 3 hepatocellular carcinoma (HCC) in a $Fah^{-/-}$, $p21^{-/-}$ mouse off NTBC. Scale bar = 50 μm.

(F) Median lobe of a $Fah^{-/-}$,$p21^{-/-}$ mouse off NTBC after clonal progression of dysplastic hepatocytes to cancer nodules.

cysts (Figure 5A) comprising large areas of the renal parenchyma (Figures 5B) within 10 weeks after NTBC withdrawal. In addition to cyst formation, renal carcinomas were present in 80% (8 of 10) of these mice after only 12 weeks of NTBC withdrawal (Figures 5C–5F). Histologically, these carcinomas corresponded to grade 2–3 of the Fuhrman classification for human renal cell carcinoma (Fuhrman et al., 1982). Clones of dysplastic renal proximal tubular cells (Figure 5C) exhibiting high proliferative activity (Figure 5D) gave rise to the renal cell carcinomas (Figures 5E and 5F). Dysplastic proliferating renal proximal tubular cells were not detected in the p21-expressing $Fah^{-/-}$ controls (data not shown). Moreover, renal carcinomas do not occur in $Fah^{-/-}$ mice, even after 1 year of low-dose NTBC treatment, which invariably causes HCCs (Figure S4C) (Al-Dhalimy et al., 2002; Grompe et al., 1995).

DISCUSSION

Our results show that p21 alone is sufficient to suppress the extraordinary regenerative capacity of hepatocytes and kidney proximal tubular cells. In the subacute or chronic injury state as modeled here, loss of p21 was not compensated by other cell-cycle inhibitors. In the absence of p21, proliferation of cells with DNA damage resulted in rapid cancer formation. The rapid development of renal and hepatic carcinomas seen here is not found in any other experimental system and suggests that p21 may be an important target for silencing in tumors derived from these tissues. In support of this hypothesis, recent clinical observations suggest that loss of p21 expression marks the transition from hepatocyte dysplasia to HCC (Plentz et al., 2007). Our finding that the antiproliferative effect of p21 is dose dependent indicates that complete abolishment of p21 by genetic mutation is not needed to unlock proliferation. Lowering the levels of p21 protein suffices, and epigenetic changes such as promoter methylation, microRNA-mediated silencing, and mechanisms regulating protein distribution and degradation may therefore cause HCCs by weakening p21-dependent cell-cycle arrest in cells with DNA damage. Such a threshold would explain findings that higher levels of p21 are associated with better prognosis in human HCCs (Kao et al., 2007).

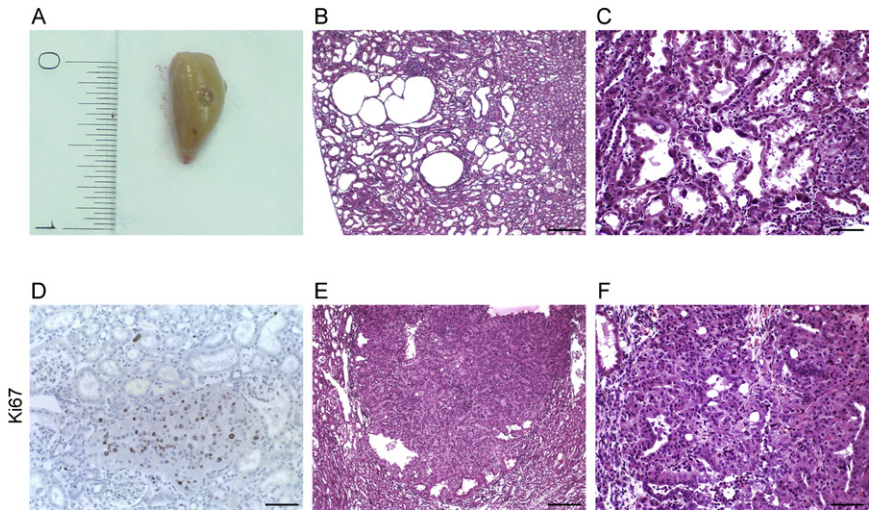

Figure 5. Unrestricted Proliferation of DNA-Damaged Renal Proximal Tubular Cells Results in Formation of Cysts and Carcinomas

(A and B) $Fah^{-/-}$,$p21^{-/-}$ mice develop renal cysts after NTBC withdrawal.

(A) Large cysts extend to the surface of the kidney (scale in inches).

(B) Cystically dilated proximal convoluted tubules and cysts. Scale bar = 200 μm.

(C–F) Progression of renal tubular dysplasia to renal carcinomas in $Fah^{-/-}$,$p21^{-/-}$ mice off NTBC.

(C) Dysplastic renal proximal tubular cells with large and hyperchromatic nuclei. Scale bar = 50 μm.

(D) Immunohistochemistry for Ki67 (brown staining) shows cluster of proliferating dysplastic renal epithelial cells. Scale bar = 50 μm.

(E) Kidney cancer nodule compressing the surrounding parenchyma. Scale bar = 100 μm.

(F) Representative H&E staining of grade 2–3 (Fuhrman classification) renal cell carcinoma. Scale bar = 50 μm.

On the other hand, we find that accumulation of p21 prevents hepatocyte regeneration and leads to liver failure and death in Fah-deficient mice. Analogously, transgenic overexpression of p21 impairs hepatocyte proliferation in liver development and after partial hepatectomy (Wu et al., 1996). Moreover, p21 has been suggested to inhibit hepatocyte regeneration in chronic human liver diseases leading to cirrhosis such as autoimmune and viral hepatitis (Lunz et al., 2005) and nonalcoholic steatohepatitis (Richardson et al., 2007). Therefore, inappropriately high levels of p21, while protective against cancer, may have adverse consequences for liver homeostasis or regeneration. Together, these findings indicate that levels of p21 protein must be tightly regulated in the liver in order to balance regenerative fitness with cancer risk.

Resistance to apoptosis has recently emerged as a factor contributing to cancer initiation and progression. Because p21 can suppress apoptosis, therapeutic strategies aimed at attenuation of p21 in malignant cells have been proposed (Weiss, 2003). Indeed, our results confirm that lack of p21 renders Fah-deficient cells susceptible to cell death. However, apoptosis failed to dispose of enough cancer-initiating cells, and the net result of p21 deficiency was increased, not decreased, carcinogenesis. Therefore, overcoming apoptosis resistance by suppression of p21 would require additional antiproliferative means. Alternatively, specific targeting of the antiapoptotic function of p21 while maintaining or enhancing its cell-cycle inhibitory capacity might be a safer and more effective anticarcinogenic strategy.

EXPERIMENTAL PROCEDURES

Mice

Fah$^{\Delta exon5}$ (129S4) (Grompe et al., 1993) and B6;129S2-*Cdkn1a*^{tm1Tyj}/J (Brugarolas et al., 1995) (The Jackson Laboratory) mice were crossed to generate *Fah*$^{-/-}$,*p21*$^{+/-}$ breeders from which all *Fah*$^{-/-}$ and *Fah*$^{-/-}$,*p21*$^{-/-}$ animals used in these studies were derived. Drinking water was supplemented with NTBC (gift from S. Lindstedt) at a concentration of 7.5 μg/ml (Grompe et al., 1995). Five percent of this normal dose was used for low-dose NTBC treatment. BrdU (Sigma) was either added to the drinking water at a concentration of 0.8 mg/ml or injected intraperitoneally at 100 μg/g. For apoptosis induction, animals were injected intraperitoneally with 0.3 μg/g of the monoclonal Fas antibody Jo2 (PharMingen). 2/3 partial hepatectomy was performed by resection of the left lateral and median liver lobe, residing below and to the left and right of the gall bladder, respectively. All animal experiments were approved by the Institutional Animal Care and Use Committee of the Oregon Health & Science University.

Microarray

Total RNA was isolated from freshly harvested liver samples using the RNeasy Protect Mini Kit (QIAGEN), and 10 μg was used for production of biotinylated antisense RNA as described previously (Golub et al., 1999). Labeled RNA was hybridized to Affymetrix 430A 2.0 or 430 2.0 oligonucleotide arrays in the Affymetrix Microarray Core of the Oregon Health & Science University (http://www.ohsu.edu/gmsr/amc/). Data analyses were performed using Affymetrix Expression Analysis software.

Histology, Immunostaining, and TUNEL Assay

Liver samples were fixed in 10% phosphate-buffered formalin (pH 7.4), dehydrated in 100% ethanol, and embedded in paraffin wax at 58°C. Sections (5 μm) were rehydrated and stained with hematoxylin and eosin (H&E). Immunohistochemistry with antibodies for BrdU (DakoCytomation), Ki67 (Novocastra), histone H3 (Ser10) (Upstate), AFP (ICN), and TUNEL assays (ApopTag, Serological Corporation) were performed as described previously (Vogel et al., 2004). For immunocytochemistry, single-cell hepatocyte suspensions were generated by liver collagenase perfusion as reported previously (Overturf et al., 1996). Hepatocytes were plated in six-well Primaria dishes (Falcon/Becton Dickinson Labware) at a density of 1×10^4 cells/cm^2. Four hours after plating, cells were fixed in 4% paraformaldehyde (Sigma) and permeabilized with 0.25% Triton X-100 (Sigma). Blocking was carried out in 10% FCS (Hyclone). For antigen detection, a goat p21 antibody (Santa Cruz Biotechnology) and an HRP-conjugated donkey anti-goat antibody (Jackson ImmunoResearch) were used. Visualization of immunocomplexes was performed with a DAB peroxidase substrate kit (Vector Laboratories), and SYBR green I (Molecular Probes) was used to dye DNA.

Caspase Activity Assay

Liver lysates were prepared by homogenization in hypotonic buffer (25 mM HEPES [pH 7.5], 5 mM $MgCl_2$, 1 mM EGTA, 1 mM phenylmethylsulfonyl fluoride). Homogenates were centrifuged at 15,000 rpm for 15 min, and 50 μg aliquots of the extracted proteins were tested in triplicate assays by measuring the proteolytic cleavage of a specific fluorogenic substrate for caspase-3 (CaspACE Assay System, Promega).

Comet Assay

Single-cell gel electrophoresis for the detection of DNA damage in mouse hepatocytes was performed according to standard procedures (Singh et al., 1988). Briefly, 10 mg of liver tissue was minced and then homogenized in buffer (75 mM NaCl, 24 mM EDTA [pH 7.5]) using a loosely fitting Potter-Elvehjem homogenizer (Bellco Glass). After sedimentation, single cells remaining in the supernatant were pelleted at 700 × g for 4 min and resuspended in buffer. Ten microliters of cellular suspension (>1×10^4 cells) was mixed with 120 μl of low-melting-point agarose at 37°C and then added to normal-melting-point agarose-coated microscope slides. The slides were immersed in cold lysing solution overnight and then placed in an electrophoresis tray with an alkaline solution (300 mM NaOH, 1 mM Na_2EDTA [pH 13]) for 10 min to allow DNA to unwind. Electrophoresis was conducted at room temperature for 15 min at 25V and 300 mA. The slides were washed, stained with ethidium bromide, and examined at 400× magnification using a fluorescence microscope. Per animal, 100 individual cells on two replicate slides were evaluated using Scion Image software (Scion) combined with an additional comet macro (gift from A. Rapp). The mean of the tail moment (DNA migration × tail intensity) was calculated as a measure of DNA damage (Hartmann et al., 2003). Differences between mean values were tested for statistical significance ($p < 0.05$) using Student's t test and one-way analysis of variance.

Western Blot

Protein extracts were resolved by SDS-PAGE and transferred onto polyvinylidene difluoride membranes (Millipore). Coomassie staining was used to demonstrate equal protein loading. Western blotting was performed as described previously (Vogel et al., 2004). Antibodies for p21, p53, c-Jun, and Mdm2 were purchased from Santa Cruz. Immunolabeled proteins were detected with a chemiluminescence kit (Bio-Rad) and Hyperfilm enhanced chemiluminescence film (Amersham Biosciences).

ACCESSION NUMBERS

Complete microarray results are available at the NCBI Gene Expression Omnibus (http://www.ncbi.nlm.nih.gov/geo/) under the accession number GSE11098.

SUPPLEMENTAL DATA

The Supplemental Data include Supplemental Experimental Procedures, one table, and four figures and can be found with this article online at http://www.cancercell.org/cgi/content/full/14/1/59/DC1/.

ACKNOWLEDGMENTS

H.W. is a Liver Scholar of the American Liver Foundation/American Society of Transplantation. A.D.S. is supported by an Alpha-1 Foundation postdoctoral fellowship. This work was supported by grants from the UCSF Institute for

Regeneration Medicine and Department of Surgery, Liver Center, and the Sandler Foundation to H.W. and from the National Institutes of Health to M.G. (R01 DK48252).

Received: February 7, 2005
Revised: March 2, 2008
Accepted: May 14, 2008
Published: July 7, 2008

REFERENCES

Albrecht, J.H., Poon, R.Y., Ahonen, C.L., Rieland, B.M., Deng, C., and Crary, G.S. (1998). Involvement of p21 and p27 in the regulation of CDK activity and cell cycle progression in the regenerating liver. Oncogene *16*, 2141–2150.

Al-Dhalimy, M., Overturf, K., Finegold, M., and Grompe, M. (2002). Long-term therapy with NTBC and tyrosine-restricted diet in a murine model of hereditary tyrosinemia type I. Mol. Genet. Metab. *75*, 38–45.

Bartosiewicz, M.J., Jenkins, D., Penn, S., Emery, J., and Buckpitt, A. (2001). Unique gene expression patterns in liver and kidney associated with exposure to chemical toxicants. J. Pharmacol. Exp. Ther. *297*, 895–905.

Bhunia, A.K., Piontek, K., Boletta, A., Liu, L., Qian, F., Xu, P.N., Germino, F.J., and Germino, G.G. (2002). PKD1 induces p21(waf1) and regulation of the cell cycle via direct activation of the JAK-STAT signaling pathway in a process requiring PKD2. Cell *109*, 157–168.

Brugarolas, J., Chandrasekaran, C., Gordon, J.I., Beach, D., Jacks, T., and Hannon, G.J. (1995). Radiation-induced cell cycle arrest compromised by p21 deficiency. Nature *377*, 552–557.

Bruix, J., Boix, L., Sala, M., and Llovet, J.M. (2004). Focus on hepatocellular carcinoma. Cancer Cell *5*, 215–219.

Calvisi, D.F., Factor, V.M., Ladu, S., Conner, E.A., and Thorgeirsson, S.S. (2004). Disruption of beta-catenin pathway or genomic instability define two distinct categories of liver cancer in transgenic mice. Gastroenterology *126*, 1374–1386.

Fuhrman, S.A., Lasky, L.C., and Limas, C. (1982). Prognostic significance of morphologic parameters in renal cell carcinoma. Am. J. Surg. Pathol. *6*, 655–663.

Gartel, A.L., and Tyner, A.L. (2002). The role of the cyclin-dependent kinase inhibitor p21 in apoptosis. Mol. Cancer Ther. *1*, 639–649.

Golub, T.R., Slonim, D.K., Tamayo, P., Huard, C., Gaasenbeek, M., Mesirov, J.P., Coller, H., Loh, M.L., Downing, J.R., Caligiuri, M.A., et al. (1999). Molecular classification of cancer: class discovery and class prediction by gene expression monitoring. Science *286*, 531–537.

Greene, A.K., and Puder, M. (2003). Partial hepatectomy in the mouse: technique and perioperative management. J. Invest. Surg. *16*, 99–102.

Grompe, M., al-Dhalimy, M., Finegold, M., Ou, C.N., Burlingame, T., Kennaway, N.G., and Soriano, P. (1993). Loss of fumarylacetoacetate hydrolase is responsible for the neonatal hepatic dysfunction phenotype of lethal albino mice. Genes Dev. *7*, 2298–2307.

Grompe, M., Lindstedt, S., al-Dhalimy, M., Kennaway, N.G., Papaconstantinou, J., Torres-Ramos, C.A., Ou, C.N., and Finegold, M. (1995). Pharmacological correction of neonatal lethal hepatic dysfunction in a murine model of hereditary tyrosinaemia type I. Nat. Genet. *10*, 453–460.

Guo, D., Fu, T., Nelson, J.A., Superina, R.A., and Soriano, H.E. (2002). Liver repopulation after cell transplantation in mice treated with retrorsine and carbon tetrachloride. Transplantation *73*, 1818–1824.

Hartmann, A., Agurell, E., Beevers, C., Brendler-Schwaab, S., Burlinson, B., Clay, P., Collins, A., Smith, A., Speit, G., Thybaud, V., and Tice, R.R. (2003). Recommendations for conducting the in vivo alkaline Comet assay. 4th International Comet Assay Workshop. Mutagenesis *18*, 45–51.

Hirohashi, S., Ishak, K.G., Kojiro, M., Wanless, I.R., Theise, N.D., Tsukuma, H., Blum, H.E., Deugnier, Y., Laurent Puig, P., Fischer, H.P., and Sakamoto, M. (2000). Hepatocellular carcinoma. In Pathology and Genetics of Tumours of the Digestive System, L.A. Aaltonen and S.R. Hamilton, eds. (Lyon, France: IARC Press), pp. 159–172.

Holme, E., and Lindstedt, S. (2000). Nontransplant treatment of tyrosinemia. Clin. Liver Dis. *4*, 805–814.

Jorquera, R., and Tanguay, R.M. (1997). The mutagenicity of the tyrosine metabolite, fumarylacetoacetate, is enhanced by glutathione depletion. Biochem. Biophys. Res. Commun. *232*, 42–48.

Jorquera, R., and Tanguay, R.M. (2001). Fumarylacetoacetate, the metabolite accumulating in hereditary tyrosinemia, activates the ERK pathway and induces mitotic abnormalities and genomic instability. Hum. Mol. Genet. *10*, 1741–1752.

Kao, J.T., Chuah, S.K., Huang, C.C., Chen, C.L., Wang, C.C., Hung, C.H., Chen, C.H., Wang, J.H., Lu, S.N., Lee, C.M., et al. (2007). P21/WAF1 is an independent survival prognostic factor for patients with hepatocellular carcinoma after resection. Liver Int. *27*, 772–781.

Lu, W., Peissel, B., Babakhanlou, H., Pavlova, A., Geng, L., Fan, X., Larson, C., Brent, G., and Zhou, J. (1997). Perinatal lethality with kidney and pancreas defects in mice with a targetted Pkd1 mutation. Nat. Genet. *17*, 179–181.

Luijerink, M.C., Jacobs, S.M., van Beurden, E.A., Koornneef, L.P., Klomp, L.W., Berger, R., and van den Berg, I.E. (2003). Extensive changes in liver gene expression induced by hereditary tyrosinemia type I are not normalized by treatment with 2-(2-nitro-4-trifluoromethylbenzoyl)-1,3-cyclohexanedione (NTBC). J. Hepatol. *39*, 901–909.

Luijerink, M.C., van Beurden, E.A., Malingre, H.E., Jacobs, S.M., Grompe, M., Klomp, L.W., Berger, R., and van den Berg, I.E. (2004). Renal proximal tubular cells acquire resistance to cell death stimuli in mice with hereditary tyrosinemia type 1. Kidney Int. *66*, 990–1000.

Lunz, J.G., 3rd, Tsuji, H., Nozaki, I., Murase, N., and Demetris, A.J. (2005). An inhibitor of cyclin-dependent kinase, stress-induced p21Waf-1/Cip-1, mediates hepatocyte mito-inhibition during the evolution of cirrhosis. Hepatology *41*, 1262–1271.

Mallet, V.O., Mitchell, C., Guidotti, J.E., Jaffray, P., Fabre, M., Spencer, D., Arnoult, D., Kahn, A., and Gilgenkrantz, H. (2002). Conditional cell ablation by tight control of caspase-3 dimerization in transgenic mice. Nat. Biotechnol. *20*, 1234–1239.

Martin-Caballero, J., Flores, J.M., Garcia-Palencia, P., and Serrano, M. (2001). Tumor susceptibility of p21(Waf1/Cip1)-deficient mice. Cancer Res. *61*, 6234–6238.

Michalopoulos, G.K., and DeFrances, M.C. (1997). Liver regeneration. Science *276*, 60–66.

Mitchell, C., Nivison, M., Jackson, L.F., Fox, R., Lee, D.C., Campbell, J.S., and Fausto, N. (2005). Heparin-binding epidermal growth factor-like growth factor links hepatocyte priming with cell cycle progression during liver regeneration. J. Biol. Chem. *280*, 2562–2568.

Montalto, G., Cervello, M., Giannitrapani, L., Dantona, F., Terranova, A., and Castagnetta, L.A. (2002). Epidemiology, risk factors, and natural history of hepatocellular carcinoma. Ann. N Y Acad. Sci. *963*, 13–20.

Overturf, K., Al-Dhalimy, M., Tanguay, R., Brantly, M., Ou, C.N., Finegold, M., and Grompe, M. (1996). Hepatocytes corrected by gene therapy are selected in vivo in a murine model of hereditary tyrosinaemia type I. Nat. Genet. *12*, 266–273.

Plentz, R.R., Park, Y.N., Lechel, A., Kim, H., Nellessen, F., Langkopf, B.H., Wilkens, L., Destro, A., Fiamengo, B., Manns, M.P., et al. (2007). Telomere shortening and inactivation of cell cycle checkpoints characterize human hepatocarcinogenesis. Hepatology *45*, 968–976.

Richardson, M.M., Jonsson, J.R., Powell, E.E., Brunt, E.M., Neuschwander-Tetri, B.A., Bhathal, P.S., Dixon, J.B., Weltman, M.D., Tilg, H., Moschen, A.R., et al. (2007). Progressive fibrosis in nonalcoholic steatohepatitis: association with altered regeneration and a ductular reaction. Gastroenterology *133*, 80–90.

Russo, P., and O'Regan, S. (1990). Visceral pathology of hereditary tyrosinemia type I. Am. J. Hum. Genet. *47*, 317–324.

Shi, Y.Z., Hui, A.M., Takayama, T., Li, X., Cui, X., and Makuuchi, M. (2000). Reduced p21(WAF1/CIP1) protein expression is predominantly related to altered p53 in hepatocellular carcinomas. Br. J. Cancer *83*, 50–55.

Singh, N.P., McCoy, M.T., Tice, R.R., and Schneider, E.L. (1988). A simple technique for quantitation of low levels of DNA damage in individual cells. Exp. Cell Res. *175*, 184–191.

van Spronsen, F.J., Bijleveld, C.M., van Maldegem, B.T., and Wijburg, F.A. (2005). Hepatocellular carcinoma in hereditary tyrosinemia type I despite 2-(2 nitro-4-3 trifluoro- methylbenzoyl)-1, 3-cyclohexanedione treatment. J. Pediatr. Gastroenterol. Nutr. *40*, 90–93.

Vogel, A., van Den Berg, I.E., Al-Dhalimy, M., Groopman, J., Ou, C.N., Ryabinina, O., Iordanov, M.S., Finegold, M., and Grompe, M. (2004). Chronic liver disease in murine hereditary tyrosinemia type 1 induces resistance to cell death. Hepatology *39*, 433–443.

Wagayama, H., Shiraki, K., Yamanaka, T., Sugimoto, K., Ito, T., Fujikawa, K., Takase, K., and Nakano, T. (2001). p21WAF1/CTP1 expression and hepatitis virus type. Dig. Dis. Sci. *46*, 2074–2079.

Weiss, R.H. (2003). p21Waf1/Cip1 as a therapeutic target in breast and other cancers. Cancer Cell *4*, 425–429.

Wu, H., Wade, M., Krall, L., Grisham, J., Xiong, Y., and Van Dyke, T. (1996). Targeted in vivo expression of the cyclin-dependent kinase inhibitor p21 halts hepatocyte cell-cycle progression, postnatal liver development and regeneration. Genes Dev. *10*, 245–260.

Zhivotovsky, B., and Kroemer, G. (2004). Apoptosis and genomic instability. Nat. Rev. Mol. Cell Biol. *5*, 752–762.

Zhou, B.P., Liao, Y., Xia, W., Spohn, B., Lee, M.H., and Hung, M.C. (2001). Cytoplasmic localization of p21Cip1/WAF1 by Akt-induced phosphorylation in HER-2/neu-overexpressing cells. Nat. Cell Biol. *3*, 245–252.